

Vapor–Liquid Equilibrium, Densities, and Interfacial Tensions of the System Ethanol + Tetrahydro-2H-pyran

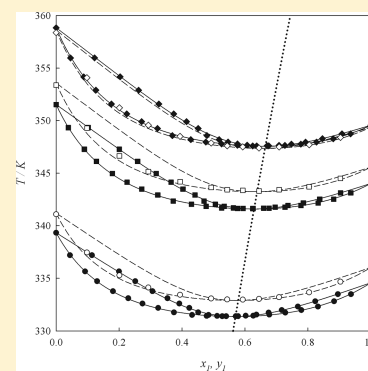
Andrés Mejía,^{*,†} Hugo Segura,^{*,†} Marcela Cartes,[†] and J. Ricardo Pérez-Correa[‡]

[†]Departamento de Ingeniería Química, Universidad de Concepción, P. O. Box 160-C, Correo 3, Concepción, Chile

[‡]Department of Chemical and Bioprocesses Engineering, Pontificia Universidad Católica de Chile, Avenida Vicuña Mackenna 4860, Santiago, Chile

S Supporting Information

ABSTRACT: Isobaric vapor–liquid equilibrium (VLE) data have been measured for the binary system ethanol + tetrahydro-2H-pyran at (50, 75, and 94) kPa and over the temperature range (331 to 358) K using a vapor–liquid equilibrium still with circulation of both phases. Mixing volumes were also determined at 298.15 K and atmospheric pressure with a vibrating tube densimeter, while a maximum differential bubble pressure tensiometer was used to measure atmospheric interfacial tensions at 303.15 K. According to experimental results, the mixture exhibits positive deviation from ideal behavior, and minimum boiling point azeotropy is present at mid-range concentrations ($0.55 < x_1^{Az} < 0.67$). VLE measurements show also that the azeotropic mole fraction impoverishes in ethanol as pressure (or temperature) increases. The mixing volumes of the mixture evolve from positive to negative deviations as the concentration of ethanol increases. Finally, it is experimentally observed that the interfacial tensions exhibit positive deviations from the linear behavior. The VLE data of the binary mixture satisfy Fredenlund's consistency test and were well-correlated by the Wohl, nonrandom two-liquid (NRTL), Wilson, and universal quasichemical (UNIQUAC) equations for all of the measured isobars. The mixing volumes and interfacial tensions, in turn, were satisfactorily correlated using the Redlich–Kister equation.



INTRODUCTION

Ethers (branched and cyclic) are considered some of the most important chemicals in the industry. Particularly, branched ethers (such as 2-methoxy-2-methylpropane or MTBE, 2-ethoxy-2-methylpropane or ETBE, 2,2'-oxybis[propane] or DIPE, and 2-methoxy-2-methylbutane or TAME) have extensively been used as oxygenates in gasoline production. Cyclic ethers, in turn (e.g., tetrahydrofuran or THF, 1,4-dioxane, and tetrahydro-2H-pyran or THP), are frequently used as solvents in chemical and electrochemical processes, as well as basic reagents (i.e., monomer) for ring-opening polymerization, and for the production of other chemical intermediaries. Recently, industrial interest in using THP as a potentially attractive cyclic ether has increased due to new and economic production routes.^{1–4}

Thermophysical properties of THP-based mixtures are useful for exploring their potential in the formulation of new alternatives for commercial fuels. In fact, detailed vapor–liquid equilibrium (VLE) data are needed for rationalizing the production of THP¹ at industrial scale, and additionally, they may provide useful information for characterizing the distillation curve (fuel concentration during vaporization) and the Reid vapor pressures (volatility indicator) for possible gasoline blending applications. Density data, in turn, are required for designing engine injection systems and for adequate vessels for fuel storage and transportation. Interfacial tension (IFT) data are needed to characterize the formation

and ignition kinetics of fuel drops. Finally, VLE, density, and IFT data are important for assessing the environmental impact of organic mixtures in air, ground, and aquifers. In fact, IFTs define the wettability patterns of fluid systems in aquifers and soils, thus providing a route to rationalize environmental remediation methods.

In spite of their potential relevance, and compared to the case of more traditional cyclic ethers,^{5–7} few experimental works have been devoted to characterize the thermophysical properties of THP mixtures. In general, we have observed that available data for THP + *n*-alkane and + alcohol mixtures are scarce and incomplete. Only Uno et al.⁸ have reported boiling temperatures and liquid phase mole fractions from (40 to 98) kPa for ethanol + THP. According to that data, the mixture exhibits positive deviation from ideal behavior, and additionally, an azeotrope is present. To the best of our knowledge, neither mixing volumes (or excess volumes, V^E) nor IFT data have been previously reported for THP-based mixtures.

This contribution is undertaken to experimentally determine new and accurate data for the phase equilibrium, mixing densities, and atmospheric interfacial tensions of ethanol + THP, thus contributing to the thermophysical characterization of THP + polar solvents.

Received: October 25, 2011

Accepted: December 14, 2011

Published: December 29, 2011

Table 1. Gas Chromatography (GC) Purities (Mass Fraction), Refractive Index (n_D) at Na D line, Densities (ρ), Normal Boiling Points (T_b), and Interfacial Tensions (σ) of Pure Components

| component (purity/mass fraction) | n_D | | $\rho/\text{g}\cdot\text{cm}^{-3}$ | | T_b/K | | $\sigma/\text{mN}\cdot\text{m}^{-1}$ | |
|----------------------------------|-----------------------|----------------------|------------------------------------|----------------------|-------------------------|---------------------|--------------------------------------|--------------------|
| | $T/\text{K} = 298.15$ | | $T/\text{K} = 298.15$ | | $p/\text{kPa} = 101.33$ | | $T/\text{K} = 303.15$ | |
| | exp. | lit. | exp. | lit. | exp. | lit. | exp. | lit. |
| ethanol (0.999) | 1.36068 | 1.35940 ^a | 0.78509 | 0.78589 ^a | 351.45 | 351.44 ^a | 21.7 | 21.68 ^a |
| THP (0.998) | 1.42000 | 1.41950 ^b | 0.87903 | 0.87880 ^c | 361.36 | 361.31 ^d | 27.1 | 26.66 ^e |

^aDaubert and Danner.⁹ ^bRiddick et al.¹⁰ ^cGiner et al.¹¹ ^dGill et al.¹² ^eInterpolated data from Villares et al.¹³

EXPERIMENTAL SECTION

Chemicals. Ethanol (Merck) and tetrahydro-2H-pyran (Aldrich) were used as received, without considering additional purification. Table 1 reports the purity of the components (as determined by gas chromatography, GC), together with the normal boiling points of the pure fluids (T_b), the mass densities (ρ), the refractive indexes (n_D) at 298.15 K, and the interfacial tensions (σ) of pure fluids at 303.15 K. The reported values are also compared with those reported in the literature.^{9–13}

Apparatus and Procedure. VLE data were determined by using an all-glass VLE cell model 601 (Fischer Labor and Verfahrenstechnik). The temperature accuracy was ± 0.02 K, whereas the pressure was measured with an estimated accuracy of ± 0.03 kPa. Densities were measured using an Anton Paar DMA 5000 vibrating U-tube densimeter. The accuracy of density measurements was $5\cdot 10^{-6}$ g·cm⁻³, and the temperature of the apparatus was maintained constant to within ± 0.01 K. The refractive indexes were measured using a multiscale automatic refractometer RFM 81 (Bellingham and Stanley). The uncertainties in measurements are $\pm 10^{-5}$, and the temperature was kept constant to within ± 0.01 K. Interfacial tensions were measured using a Sensadyne maximum differential bubble pressure tensiometer model PC500-LV. The temperature of the sample in the vessel was kept constant to within ± 0.01 K using a Julabo thermostatic bath, conditions in which interfacial tension measurements were accurate within ± 0.01 mN·m⁻¹. Specific details concerning the experimental procedures have been described in depth in recent works;^{14–17} so briefly, we constrain our description to key operating parameters. Temperature conditions in gas chromatography were (373.15, 393.15, and 493.15) K for column, injector, and detector, respectively, conditions in which concentration measurement accuracies were better than ± 0.001 in mole fraction. Additional details concerning to the VLE technique have been extensively described by Raal and Mühlbauer,¹⁸ whereas maximum differential bubble pressure technique have been described by Adamson and Gast¹⁹ and Rusanov and Prokhorov.²⁰

RESULTS AND DISCUSSION

Vapor–Liquid Equilibrium. The boiling temperature T , the liquid x_i and vapor-phase y_i mole fractions of component i at $P = (50, 75, \text{ and } 94)$ kPa are reported in Tables 2 to 4 and illustrated in Figure 1 (solid symbols). Tables 2 to 4 also include the activity coefficients (γ_i), which are displayed in Figures S1 to S3 in the Supporting Information and were calculated from the following equation:²¹

$$\ln \gamma_i = \ln \frac{y_i P}{x_i P_i^0} + \frac{(B_{ii} - V_i^L)(P - P_i^0)}{RT} + y_j^2 \frac{\delta_{ij} P}{RT} \quad (1)$$

Table 2. Experimental VLE Data for Ethanol (1) + THP (2) at $P = 50.00$ kPa^a

| T K | x_1 | y_1 | γ_1 | γ_2 | $-B_{ij}/\text{cm}^3\cdot\text{mol}^{-1}$ | | |
|----------|-------|-------|------------|------------|---|------|-----|
| | | | | | 11 | 22 | 12 |
| 339.33 | 0.000 | 0.000 | | 1.000 | | 1258 | |
| 337.19 | 0.044 | 0.114 | 2.346 | 0.998 | 1170 | 1279 | 710 |
| 335.65 | 0.092 | 0.200 | 2.095 | 1.001 | 1196 | 1295 | 718 |
| 334.72 | 0.130 | 0.251 | 1.939 | 1.011 | 1212 | 1305 | 723 |
| 333.77 | 0.181 | 0.306 | 1.770 | 1.029 | 1229 | 1315 | 728 |
| 333.11 | 0.229 | 0.354 | 1.658 | 1.044 | 1241 | 1322 | 732 |
| 332.60 | 0.275 | 0.391 | 1.565 | 1.064 | 1250 | 1328 | 734 |
| 332.19 | 0.324 | 0.423 | 1.458 | 1.100 | 1257 | 1332 | 737 |
| 331.77 | 0.375 | 0.452 | 1.371 | 1.148 | 1265 | 1337 | 739 |
| 331.52 | 0.432 | 0.484 | 1.288 | 1.200 | 1270 | 1340 | 740 |
| 331.43 | 0.479 | 0.512 | 1.233 | 1.242 | 1271 | 1341 | 741 |
| 331.40 | 0.528 | 0.540 | 1.181 | 1.293 | 1272 | 1341 | 741 |
| 331.40 | 0.578 | 0.571 | 1.138 | 1.354 | 1272 | 1341 | 741 |
| 331.45 | 0.627 | 0.602 | 1.106 | 1.414 | 1271 | 1341 | 741 |
| 331.55 | 0.678 | 0.636 | 1.075 | 1.493 | 1269 | 1340 | 740 |
| 331.74 | 0.728 | 0.675 | 1.052 | 1.574 | 1266 | 1337 | 739 |
| 331.99 | 0.779 | 0.717 | 1.032 | 1.675 | 1261 | 1335 | 738 |
| 332.31 | 0.832 | 0.768 | 1.020 | 1.786 | 1255 | 1331 | 736 |
| 332.82 | 0.883 | 0.824 | 1.007 | 1.922 | 1246 | 1326 | 733 |
| 333.49 | 0.937 | 0.896 | 1.002 | 2.069 | 1234 | 1318 | 730 |
| 334.57 | 1.000 | 1.000 | 1.000 | | 1214 | | |

^a T is the equilibrium temperature; x_i and y_i are mole fractions in liquid and vapor phases of component i , respectively. γ_i are the activity coefficients of component i , and B_{ij} are the molar virial coefficients.

where P is the total pressure and P_i^0 is the pure component vapor pressure. R is the universal gas constant. V_i^L is the liquid molar volume of component i , B_{ii} and B_{jj} are the second virial coefficients of the pure gases, B_{ij} is the cross second virial coefficient, and the mixing rule of second virial coefficients (δ_{ij}) is given by $\delta_{ij} = 2B_{ij} - B_{jj} - B_{ii}$.

Equation 1 is valid from low to moderate pressures, where the virial equation of state truncated after the second term is adequate for describing the vapor phase of the pure components and their mixtures and, additionally, the liquid molar volumes of pure components are incompressible over the pressure range under consideration. Liquid molar volumes were estimated from the correlation proposed by Rackett.²² Critical properties were taken from Riddick et al.¹⁰ The molar virial coefficients B_{ii} , B_{jj} , and B_{ij} were estimated by the method of Hayden and O'Connell²³ using the molecular and solvation parameters η suggested by Prausnitz et al.²⁴ for ethanol. For the case of THP, molecular parameters and physical properties were also taken from ref 10. THP's solvation parameter η was estimated by smoothing experimental data of second virial coefficients reported in ref 25, thus yielding the value $\eta = 0.05$. Pure component and cross virial coefficients are reported in Tables 2 to 4.

Table 3. Experimental VLE Data for Ethanol (1) + THP (2) at $P = 75.00$ kPa^a

| T | | x_1 | y_1 | γ_1 | γ_2 | $-B_{ij}/\text{cm}^3\cdot\text{mol}^{-1}$ | | |
|--------|-------|-------|-------|------------|------------|---|-----|------|
| K | | | | | | 11 | 22 | 12 |
| 351.53 | 0.000 | 0.000 | | | 1.000 | | | 1145 |
| 349.33 | 0.038 | 0.102 | 2.190 | 1.000 | 993 | 1164 | 651 | |
| 347.28 | 0.090 | 0.200 | 1.992 | 1.004 | 1020 | 1182 | 660 | |
| 346.13 | 0.128 | 0.259 | 1.882 | 1.009 | 1035 | 1193 | 665 | |
| 344.97 | 0.178 | 0.318 | 1.735 | 1.023 | 1051 | 1203 | 671 | |
| 344.14 | 0.225 | 0.365 | 1.629 | 1.039 | 1063 | 1211 | 675 | |
| 343.49 | 0.272 | 0.403 | 1.526 | 1.063 | 1072 | 1217 | 678 | |
| 342.92 | 0.323 | 0.441 | 1.439 | 1.091 | 1081 | 1223 | 681 | |
| 342.34 | 0.372 | 0.470 | 1.360 | 1.138 | 1089 | 1228 | 684 | |
| 342.04 | 0.430 | 0.506 | 1.283 | 1.181 | 1094 | 1231 | 685 | |
| 341.84 | 0.477 | 0.534 | 1.231 | 1.222 | 1097 | 1233 | 686 | |
| 341.70 | 0.526 | 0.563 | 1.182 | 1.272 | 1099 | 1234 | 687 | |
| 341.65 | 0.577 | 0.594 | 1.139 | 1.327 | 1100 | 1235 | 687 | |
| 341.64 | 0.626 | 0.625 | 1.103 | 1.391 | 1100 | 1235 | 687 | |
| 341.67 | 0.676 | 0.659 | 1.075 | 1.459 | 1099 | 1235 | 687 | |
| 341.77 | 0.727 | 0.696 | 1.051 | 1.541 | 1098 | 1234 | 687 | |
| 341.92 | 0.778 | 0.737 | 1.033 | 1.631 | 1095 | 1232 | 686 | |
| 342.16 | 0.833 | 0.786 | 1.019 | 1.754 | 1092 | 1230 | 685 | |
| 342.52 | 0.882 | 0.838 | 1.010 | 1.866 | 1087 | 1226 | 683 | |
| 343.12 | 0.936 | 0.904 | 1.001 | 2.011 | 1078 | 1221 | 680 | |
| 344.02 | 1.000 | 1.000 | 1.000 | | 1065 | | | |

^aT is the equilibrium temperature; x_i and y_i are mole fractions in liquid and vapor phases of component i , respectively. γ_i are the activity coefficients of component i , and B_{ij} are the molar virial coefficients.

Table 4. Experimental VLE Data for Ethanol (1) + THP (2) at $P = 94.00$ kPa^a

| T | | x_1 | y_1 | γ_1 | γ_2 | $-B_{ij}/\text{cm}^3\cdot\text{mol}^{-1}$ | | |
|--------|-------|-------|-------|------------|------------|---|-----|------|
| K | | | | | | 11 | 22 | 12 |
| 358.85 | 0.000 | 0.000 | | | 1.000 | | | 1085 |
| 355.97 | 0.046 | 0.122 | 2.123 | 1.001 | 913 | 1108 | 621 | |
| 354.17 | 0.088 | 0.203 | 1.971 | 1.004 | 934 | 1123 | 629 | |
| 352.91 | 0.126 | 0.262 | 1.851 | 1.009 | 949 | 1133 | 635 | |
| 351.58 | 0.176 | 0.326 | 1.737 | 1.018 | 965 | 1145 | 641 | |
| 350.65 | 0.225 | 0.374 | 1.612 | 1.036 | 976 | 1153 | 645 | |
| 349.91 | 0.272 | 0.414 | 1.519 | 1.056 | 985 | 1159 | 648 | |
| 349.26 | 0.322 | 0.451 | 1.429 | 1.086 | 994 | 1165 | 651 | |
| 348.58 | 0.369 | 0.479 | 1.357 | 1.133 | 1002 | 1171 | 654 | |
| 348.20 | 0.428 | 0.518 | 1.284 | 1.171 | 1007 | 1174 | 656 | |
| 347.97 | 0.476 | 0.546 | 1.228 | 1.213 | 1011 | 1176 | 657 | |
| 347.79 | 0.526 | 0.576 | 1.180 | 1.260 | 1013 | 1178 | 658 | |
| 347.66 | 0.576 | 0.607 | 1.139 | 1.314 | 1015 | 1179 | 658 | |
| 347.60 | 0.625 | 0.638 | 1.105 | 1.374 | 1015 | 1179 | 659 | |
| 347.60 | 0.676 | 0.670 | 1.074 | 1.447 | 1015 | 1179 | 659 | |
| 347.65 | 0.727 | 0.708 | 1.053 | 1.519 | 1015 | 1179 | 658 | |
| 347.77 | 0.778 | 0.748 | 1.032 | 1.613 | 1013 | 1178 | 658 | |
| 347.96 | 0.828 | 0.793 | 1.020 | 1.700 | 1011 | 1176 | 657 | |
| 348.28 | 0.881 | 0.846 | 1.010 | 1.811 | 1006 | 1173 | 655 | |
| 348.75 | 0.936 | 0.908 | 1.002 | 1.984 | 1000 | 1169 | 653 | |
| 349.56 | 1.000 | 1.000 | 1.000 | | 990 | | | |

^aT is the equilibrium temperature; x_i and y_i are mole fractions in liquid and vapor phases of component i , respectively. γ_i are the activity coefficients of component i , and B_{ij} are the molar virial coefficients.

The vapor pressures of pure components were experimentally determined as a function of temperature using the same equipment as that for obtaining the VLE data. Table 5 reports

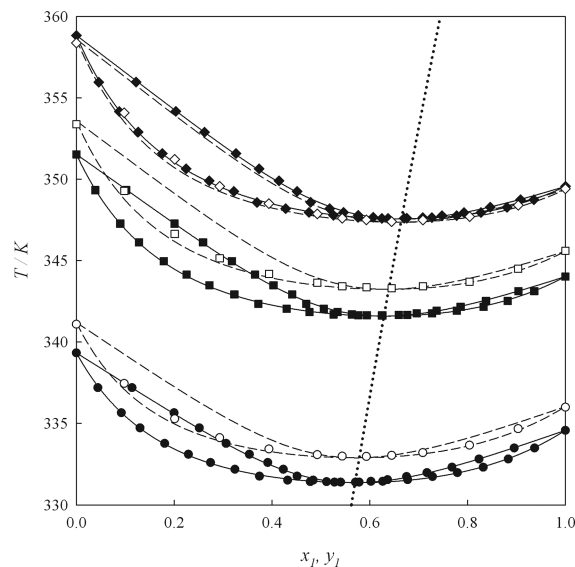


Figure 1. Isobaric phase diagram for the system ethanol (1) + THP (2). Experimental data at \bullet , 50.0 kPa; \blacksquare , 75.0 kPa; \blacklozenge , 94.0 kPa. Experimental data reported by Uno et al.⁸ at \circ , 53.33 kPa; \square , 79.99 kPa; \diamond , 93.32 kPa; —, predicted from the two-parameter Legendre polynomial used in consistency analysis; - - -, predicted from the Wohl model with the parameters indicated in Table 8; \cdots , azeotropic line.

Table 5. Experimental Vapor Pressures (P) as a Function of Temperature (T) for THP

| T/K | P/kPa |
|--------|-------|
| 312.59 | 18.01 |
| 319.62 | 24.01 |
| 325.36 | 30.01 |
| 331.70 | 38.0 |
| 336.40 | 45.0 |
| 339.98 | 51.0 |
| 344.26 | 59.0 |
| 347.64 | 66.0 |
| 350.74 | 73.0 |
| 353.61 | 80.0 |
| 356.29 | 87.0 |
| 358.81 | 94.0 |
| 361.55 | 102.1 |

Table 6. Estimated Azeotropic Coordinates for the System Ethanol (1) + THP (2)^a

| P/kPa | x_1^{Az} | T^{Az}/K |
|-------|-------------------|--------------------------|
| 50.00 | 0.570 | 331.37 |
| 75.00 | 0.629 | 341.59 |
| 94.00 | 0.665 | 347.56 |

^aP is the pressure of the system; x_1^{Az} is the azeotropic mole fraction, and T^{Az} is the azeotropic temperature.

the experimental values obtained for the vapor pressures of THP, whose dependence on temperature can be accurately correlated by using the Antoine equation:

$$\log(P_i^0/\text{kPa}) = 5.60624 - 1010.3546/[(T/\text{K}) - 80.7458] \quad (2)$$

Equation 2 correlates P_i^0 data of THP from (321.59 to 360) K with an average of the absolute percentage deviation (AAPD)

Table 7. Consistency Test Statistics for the Binary System Ethanol (1) + THP (2)

| P/kPa | L_1^a | L_2^a | 100 Δy^b | δP^c /kPa |
|-------|---------|---------|------------------|-------------------|
| 50.00 | 0.8442 | -0.0425 | 0.3 | 0.1 |
| 75.00 | 0.8044 | -0.0201 | 0.2 | 0.1 |
| 94.00 | 0.7858 | -0.0105 | 0.3 | 0.2 |

^aParameters for the Legendre polynomial²⁸ used for consistency.

^bAverage absolute deviation in vapor-phase mole fractions $\Delta y = (1/N) \sum_{i=1}^N |y_i^{\text{exp}} - y_i^{\text{cal}}|$ (N : number of data points). ^cAverage absolute deviation in vapor pressure $\delta P = (1/N) \sum_{i=1}^N |P_i^{\text{exp}} - P_i^{\text{cal}}|$.

of 0.30 %. The reliability of eq 2 for predicting vapor pressures of THP has been successfully tested against the data reported by Miyano et al.²⁶ with an AAPD of 0.5 %. For the case of ethanol, experimental vapor pressures have been previously reported,¹⁴ and their temperature dependence was obtained from:¹⁴

$$\log(P_i^0/\text{kPa}) = 7.16178 - 1549.6973/[(T/\text{K}) - 50.890] \quad (3)$$

The experimental data reported in Tables 2 to 4 allow the conclusion that the binary mixture exhibits positive deviation from ideal behavior and azeotropic behavior is present for each isobar. From Figure 1 we can conclude a good coherency between the present VLE data and those reported by Uno et al.⁸ Azeotropic concentrations of the measured binary were estimated by fitting the empirical function

$$f(x) = 100 \left(\frac{y-x}{x} \right) \quad (4)$$

where x and y have been taken from the experimental data. Azeotropic concentrations, as determined by solving $f(x) = 0$, are indicated in Table 6, where it is concluded that the mole fraction of the azeotrope impoverishes in ethanol as pressure (or temperature) increases, as it is shown in Figure 1. As it was observed with the general trend of the VLE data, the reported azeotropic coordinates are in good agreement with results presented by Uno et al.⁸

The VLE data reported in Tables 2 to 4 were found to be thermodynamically consistent by the point-to-point method of

Table 9. Densities (ρ) and Excess Volumes (V^E) as a Function of the Liquid Mole Fraction (x_1) for the Binary System Ethanol (1) + THP (2) at 298.15 K and 101.3 kPa

| x_1 | ρ | $10^3 V^E$ |
|-------|--------------------|------------------------------------|
| | g·cm ⁻³ | cm ³ ·mol ⁻¹ |
| 0.000 | 0.87903 | 0 |
| 0.030 | 0.87714 | 19 |
| 0.115 | 0.87186 | 41 |
| 0.193 | 0.86685 | 45 |
| 0.299 | 0.85954 | 40 |
| 0.426 | 0.84989 | 24 |
| 0.496 | 0.84401 | 14 |
| 0.599 | 0.83465 | 0 |
| 0.716 | 0.82274 | -11 |
| 0.799 | 0.81313 | -15 |
| 0.910 | 0.79860 | -12 |
| 0.959 | 0.79141 | -6 |
| 1.000 | 0.78511 | 0 |

Van Ness et al.²⁷ as modified by Fredenslund et al.²⁸ For each isobaric condition, the consistency criterion ($\Delta y < 0.01$) was met by fitting the equilibrium vapor pressure according to Barker's²⁹ reduction method. Statistical analysis³⁰ reveals that a two-parameter Legendre polynomial is adequate for fitting the equilibrium vapor pressure in each case. Pertinent consistency statistics and Legendre polynomial parameters are presented in Table 7. The activity coefficients presented in Tables 2 and 4 are estimated to be accurate to within 0.9 %.

The VLE data reported in Tables 2 to 4 were correlated with the Wohl, nonrandom two-liquid (NRTL), Wilson, and universal quasichemical (UNIQUAC) equations,³¹ whose adjustable parameters were obtained by minimizing the following objective function (OF):

$$\text{OF} = \sum_{i=1}^N (|P_i^{\text{exp}} - P_i^{\text{cal}}|/P_i^{\text{exp}} + |y_i^{\text{exp}} - y_i^{\text{cal}}|)^2 \quad (5)$$

In eq 5, the superscript exp stands for experimental data, while cal means calculated quantity. N is the number of data points. The parameters of the different activity coefficient models are reported in Table 8, together with the relative

Table 8. Parameters and Prediction Statistics for Different Gibbs Excess (G^E) Models in Ethanol (1) + THP (2)^a

| model | P/kPa | A_{12} | A_{21} | α_{12} | bubble-point pressures | | dew-point pressures | |
|----------------------|-------|----------|----------|--------------------|-----------------------------|--------------------|-----------------------------|--------------------|
| | | | | | ΔP (%) ^b | 100 Δy_i^c | ΔP (%) ^b | 100 Δx_i^c |
| Wohl | 50.0 | 0.911 | 0.781 | 1.448 ^d | 0.3 | 0.2 | 0.3 | 0.2 |
| | 75.0 | 0.837 | 0.752 | 1.516 ^d | 0.2 | 0.1 | 0.3 | 0.1 |
| | 94.0 | 0.804 | 0.735 | 1.568 ^d | 0.2 | 0.1 | 0.2 | 0.1 |
| NRTL | 50.0 | 732.06 | 1915.30 | 0.400 ^e | 0.3 | 0.2 | 0.3 | 0.2 |
| | 75.0 | 820.80 | 1753.95 | 0.400 ^e | 0.3 | 0.1 | 0.3 | 0.2 |
| | 94.0 | 837.97 | 1705.52 | 0.400 ^e | 0.2 | 0.1 | 0.3 | 0.1 |
| Wilson ^f | 50.0 | 3231.40 | -506.80 | | 0.3 | 0.2 | 0.3 | 0.3 |
| | 75.0 | 3097.38 | -458.91 | | 0.3 | 0.2 | 0.3 | 0.2 |
| | 94.0 | 3056.91 | -455.12 | | 0.2 | 0.2 | 0.3 | 0.2 |
| UNIQUAC ^g | 50.0 | -764.81 | 2224.63 | | 0.3 | 0.2 | 0.3 | 0.2 |
| | 75.0 | -739.41 | 2143.85 | | 0.3 | 0.1 | 0.3 | 0.2 |
| | 94.0 | -743.41 | 2130.02 | | 0.2 | 0.1 | 0.3 | 0.1 |

^a A_{12} and A_{21} are the G^E model parameters in J·mol⁻¹. ^b $\Delta P = (100/N) \sum_{i=1}^N |P_i^{\text{exp}} - P_i^{\text{cal}}|/P_i^{\text{exp}}$. ^c $\Delta \delta = 1/N \sum_{i=1}^N |\delta_i^{\text{exp}} - \delta_i^{\text{cal}}|$ with $\delta = y$ or x . ^d q parameter for the Wohl model. ^e α_{12} parameter for the NRTL model. ^fLiquid molar volumes have been estimated from the Rackett equation.²² ^gThe molecular parameters r and q are those reported in DECHEMA:⁵ $r_1 = 2.1055$, $r_2 = 3.6159$, $q_1 = 1.9720$, $q_2 = 2.9400$.

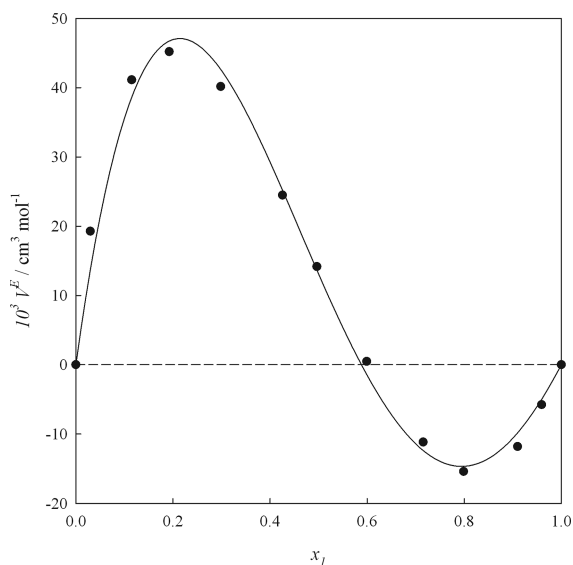


Figure 2. Excess volumes (V^E) as a function of the liquid phase (x_1) for the system ethanol (1) + THP (2) at 298.15 K and 101.3 kPa. ●, Experimental data; —, smoothed by the three-parameter Redlich–Kister expansion (see eq 7).

Table 10. Interfacial Tensions (σ) as a Function of the Liquid Mole Fraction (x_1) for the Binary System Ethanol (1) + THP (2) at 303.15 K and 101.3 kPa

| x_1 | σ |
|-------|-------------------------------|
| | $\text{mN}\cdot\text{m}^{-1}$ |
| 0.000 | 27.10 |
| 0.068 | 26.91 |
| 0.122 | 26.76 |
| 0.223 | 26.50 |
| 0.323 | 25.98 |
| 0.420 | 25.34 |
| 0.520 | 24.90 |
| 0.604 | 24.35 |
| 0.622 | 24.24 |
| 0.657 | 24.07 |
| 0.707 | 23.81 |
| 0.722 | 23.64 |
| 0.821 | 23.01 |
| 0.918 | 22.42 |
| 0.963 | 22.00 |
| 1.000 | 21.70 |

deviation for the case of bubble- and dew-point pressures. From the results presented in Table 8, it is possible to conclude that all of the fitted models gave a reasonable correlation of the binary system and that the best fit is obtained with the Wohl model. The capability of simultaneously predicting the bubble- and dew-point pressures and the vapor- and liquid-phase mole fractions, respectively, has been used as the ranking factor. To establish the coherency of the present binary data and to test the predictive capability of the parameters reported in Table 8, we have used the best-ranked model (Wohl's model) to predict available VLE data. As it is illustrated in Figure 1, the quoted Wohl's parameters predict with fair accuracy the isobaric (T, x) data reported by Uno et al.⁸ (open symbols).

According to the previous results, we can conclude that the Gibbs excess (G^E) parameters reported in this work can be used

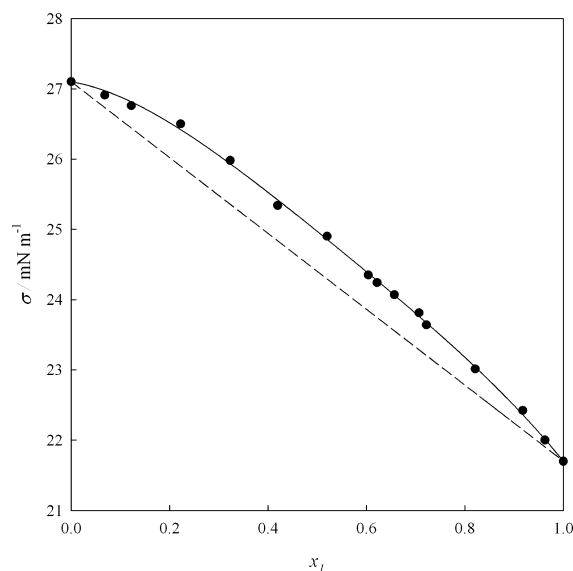


Figure 3. Interfacial tension (σ) as a function of the liquid mole fraction (x_1) for the system ethanol (1) + THP (2) at 303.15 K and 101.3 kPa. ●, experimental data; - - -, linear behavior ($x_1\sigma_1 + x_2\sigma_2$); —, smoothed by the three-parameter Redlich–Kister expansion (see eq 8).

to accurately and consistently predict the VLE of the binary system.

Excess Volume Data. Table 9 reports the experimental density data for the mixture and its pure constituents at $T = 298.15$ K and $P = 101.3$ kPa. These density data allow calculating the excess volumes (V^E) of the mixture according to

$$V^E = \frac{x_1 M_1 + x_2 M_2}{\rho} - x_1 \frac{M_1}{\rho_1} - x_2 \frac{M_2}{\rho_2} \quad (6)$$

In eq 6, ρ is the mass density of the mixture, while ρ_i corresponds to the mass density of the pure components (that have been reported in Table 1) and M_i is the molecular weight of the constituents that were taken from refs 9 and 10. The calculated V^E are estimated accurate to within $\pm 10^{-3}$ $\text{cm}^3\cdot\text{mol}^{-1}$.

According to the results presented in Table 9 and Figure 2, it is possible to conclude that the excess volumes of the system are almost negligible, showing a sharp change from a slight positive to negative deviation as the concentration of ethanol increases. To assess the coherency of their trend, V^E data have been correlated by using a three-parameter Redlich–Kister expansion:³²

$$\begin{aligned} (V^E/\text{cm}^3\cdot\text{mol}^{-1}) &= x_1 x_2 [0.052384 + 0.320883(x_2 - x_1) \\ &\quad + 0.13493(x_2 - x_1)^2] \end{aligned} \quad (7)$$

The model reported in eq 7 is characterized by a maximum deviation of $3.0\cdot 10^{-5}$ $\text{cm}^3\cdot\text{mol}^{-1}$, an average deviation of $4.0\cdot 10^{-6}$ $\text{cm}^3\cdot\text{mol}^{-1}$, and a standard deviation of $8.0\cdot 10^{-6}$ $\text{cm}^3\cdot\text{mol}^{-1}$.

Interfacial Tension Data. The interfacial tension measurements for the mixture and its pure constituents at $T = 303.15$ K and $P = 101.3$ kPa are reported in Table 10 and in Figure 3. Experimental data were correlated using a three-parameter Redlich–Kister expansion:³³

$$\begin{aligned}
 (\sigma/\text{mN}\cdot\text{m}^{-1}) = & x_1x_2[2.2793 + 0.5220(x_2 - x_1) \\
 & + 1.4316(x_2 - x_1)^2] + \\
 & (x_1\sigma_1 + x_2\sigma_2)
 \end{aligned}
 \quad (8)$$

Equation 8 yields a maximum deviation of $6.6\cdot 10^{-3}$ $\text{mN}\cdot\text{m}^{-1}$ and an average deviation and a standard deviation of $2.1\cdot 10^{-3}$ $\text{mN}\cdot\text{m}^{-1}$. From Figure 3, it is possible to conclude that the interfacial tensions of the mixture ethanol + THP exhibit positive deviations from the lineal behavior ($x_1\sigma_1 + x_2\sigma_2$).

CONCLUSIONS

Isobaric VLE data at (50, 75, and 94) kPa, atmospheric mixing volumes at 298.15 K, and interfacial tensions at 303.15 K have been measured for ethanol + THP. Experimental VLE data reveal that the binary mixture exhibits positive deviations from ideal behavior and azeotropic behavior is present. The mole fraction of the azeotrope decreases in ethanol as the pressure (or temperature) increases, in good agreement with previous measurements.⁸ Excess volumes exhibit a change from a slight positive to a negative deviation from the ideal behavior as the concentration of ethanol increases, while interfacial tensions exhibit positive deviations from the linear behavior.

The activity coefficients and boiling points of ethanol + THP were well-correlated with the liquid-phase mole fraction using the Wohl, NRTL, Wilson, and UNIQUAC equations, the best fit corresponding to the Wohl model. The excess volumes and interfacial tensions of the quoted mixture were smoothed and well-represented by the Redlich–Kister equation.

ASSOCIATED CONTENT

Supporting Information

Figures S1 to S3, which illustrate the activity coefficient plot for the system ethanol (1) + THP (2) at (50.0, 75.0, and 94.0) kPa, respectively. This material is available free of charge via the Internet at <http://pubs.acs.org>.

AUTHOR INFORMATION

Corresponding Author

*E-mail: amejia@udec.cl and hsegura@udec.cl.

Funding

This work was financed by FONDECYT, Santiago, Chile (Project 1100357).

REFERENCES

- (1) Showa Denko, K. K. Japanese Patent Disclosure WO2006062211, 2006.
- (2) Karas, L.; Piel, W. J. Ethers. In *Kirk-Othmer Encyclopedia of Chemical Technology*; John Wiley & Sons, Inc.: New York, 2004.
- (3) Sakuth, M.; Mensing, T.; Schuler, J.; Heitmann, W.; Strehlke, G. Ethers, Aliphatic. In *Ullmann's Encyclopedia of Industrial Chemistry*; Wiley: New York, 2010.
- (4) Müller, H. Tetrahydrofuran. *Ullmann's Encyclopedia of Industrial Chemistry*; Wiley: New York, 2010.
- (5) *DECHEMA Database*. Dechema Gesellschaft für Chemische Technik und Biotechnologie e.V., Frankfurt am Main, Germany; <https://cdsdt.dl.ac.uk/detherm/> (retrieved Nov 2010).
- (6) Wohlfarth, Ch.; Wohlfarth, B. Numerical Data and Functional Relationships in Science and Technology. In *Surface Tension of Pure Liquids and Binary Liquid Mixtures*, Vol. 16; Lechner, M. D., Ed.; Landolt-Börnstein, New Series Group IV Physical Chemistry; Springer Verlag: Berlin, 1997.
- (7) Wohlfarth, Ch.; Wohlfarth, B. Numerical Data and Functional Relationships in Science and Technology. In *Surface Tension of Pure Liquids and Binary Liquid Mixtures*, Vol. 24; Lechner, M. D., Ed.; Landolt-Börnstein, New Series Group IV Physical Chemistry; Springer Verlag: Berlin, 2008.
- (8) Uno, S.; Matsuda, H.; Kurihara, K.; Tochigi, K.; Miyano, Y.; Kato, S.; Yasuda, H. Isobaric Vapor-Liquid Equilibria for Tetrahydropyran and Alcohol Systems. *J. Chem. Eng. Data* **2008**, *53*, 2066–2071.
- (9) Daubert, T. E.; Danner, R. P. Physical and Thermodynamic Properties of Pure Chemicals. *Data Compilation*; Taylor and Francis: Bristol, PA, 1989.
- (10) Riddick, J. A.; Bunger, W. B.; Sakano, T. K. Organic Solvents. In *Physical Properties and Methods of Purification*; Techniques of Chemistry, Vol. II, 4rd ed.; Wiley-Interscience: New York, 1986.
- (11) Giner, I.; Montano, D.; Haro, M.; Artigas, H.; Lafuente, C. Study of isobaric vapour-liquid equilibrium of some cyclic ethers with 1-chloropropane: Experimental results and SAFT-VR modelling. *Fluid Phase Equilib.* **2009**, *278*, 62–67.
- (12) Gill, B. K.; Rattan, V. K.; Kapoor, S. Experimental Isobaric Vapor–Liquid Equilibrium Data for Binary Mixtures of Cyclic Ethers with (1- Methylene)benzene. *J. Chem. Eng. Data* **2008**, *53*, 2041–2043.
- (13) Villares, A.; Sanz, L.; Giner, B.; Lafuente, C.; López, M. C. Study of the Surface Tension of Chlorocyclohexane or Bromocyclohexane with Some Cyclic Ethers. *J. Chem. Eng. Data* **2005**, *50*, 1334–1337.
- (14) Mejía, A.; Segura, H.; Cartes, M. Vapor–Liquid Equilibria and Interfacial Tensions of the System Ethanol + 2-Methoxy-2-methylpropane. *J. Chem. Eng. Data* **2010**, *55*, 428–434.
- (15) Mejía, A.; Cartes, M.; Segura, H. Interfacial tensions of binary mixtures of ethanol with octane, decane, dodecane and tetradecane. *J. Chem. Thermodyn.* **2011**, *43*, 1395–1400.
- (16) Mejía, A.; Segura, H.; Cartes, M. Vapor–liquid equilibria and interfacial tensions of the system ethanol + 2-methoxy-2-methylbutane. *J. Chem. Eng. Data* **2011**, *56*, 3142–3148.
- (17) Mejía, A.; Segura, H.; Cartes, M. Measurement and theoretical prediction of the vapor–liquid equilibrium, densities and interfacial tensions of the system hexane + 2-methoxy-2-methylbutane. *Fluid Phase Equilib.* **2011**, *308*, 15–24.
- (18) Raal, J. D.; Mühlbauer, A. L. *Phase Equilibria: Measurement and Computation*; Series in Chemical and Mechanical Engineering; Taylor & Francis: London, 1997.
- (19) Adamson, A. W.; Gast, A. P. *Physical Chemistry of Surfaces*, 6th ed.; Wiley Interscience: New York, 1997.
- (20) Rusanov, A. I.; Prokhorov, V. A. *Interfacial Tensiometry*; Elsevier: Amsterdam, 1996.
- (21) Van Ness, H. C.; Abbott, M. M. *Classical Thermodynamics of Nonelectrolyte Solutions*; McGraw-Hill Book Co.: New York, 1982.
- (22) Rackett, H. G. Equation of state for saturated liquids. *J. Chem. Eng. Data* **1970**, *15*, 514–517.
- (23) Hayden, J.; O'Connell, J. A generalized method for predicting second virial coefficients. *Ind. Eng. Chem. Process Des. Dev.* **1975**, *14*, 209–216.
- (24) Prausnitz, J. M.; Anderson, T.; Grens, E.; Eckert, C.; Hsieh, R.; O'Connell, J. *Computer Calculations for Multicomponent Vapor–Liquid and Liquid–Liquid Equilibria*; Prentice Hall: New York, 1980.
- (25) *NIST Standard Reference Database v. 103a*; National Institute of Standards and Technology: Gaithersburg, MD, 2010.
- (26) Miyano, Y.; Uno, S.; Tochigi, K.; Kato, S.; Yasuda, H. Henry's Law Constants and Infinite Dilution Activity Coefficients of Propane, Propene, Butane, 2-Methylpropane, 1-Butene, 2-Methylpropene, trans-2-Butene, cis-2-Butene, 1,3-Butadiene, Dimethylether, Chloroethane, 1,1-Difluoroethane, and Hexane in Tetrahydropyran. *J. Chem. Eng. Data* **2007**, *52*, 2245–2249.
- (27) Van Ness, H. C.; Byer, S. M.; Gibbs, R. E. Vapor–liquid equilibrium: Part I. An appraisal of data reduction methods. *AIChE J.* **1973**, *19*, 238–244.
- (28) Fredenslund, A.; Gmehling, J.; Rasmussen, P. *Vapor-Liquid Equilibria Using UNIFAC, A Group Contribution Method*; Elsevier: Amsterdam, 1977.

(29) Barker, J. A. Determination of Activity Coefficients from total pressure measurements. *Aust. J. Chem.* **1953**, *6*, 207–210.

(30) Wisniak, J.; Apelblat, A.; Segura, H. An Assessment of Thermodynamic Consistency Tests for Vapor-Liquid Equilibrium Data. *Phys. Chem Liq.* **1997**, *35*, 1–58.

(31) Prausnitz, J. M.; Lichtenthaler, R. N.; Gomes de Azevedo, E. *Molecular Thermodynamics of Fluid-Phase Equilibria*, 3rd ed.; Prentice-Hall: Upper Saddle River, NJ, 1999.

(32) Redlich, O.; Kister, A. T. Thermodynamics of nonelectrolyte solutions - x-y-t relations in a binary system. *Ind. Eng. Chem.* **1948**, *40*, 341–345.

(33) Myers, D. B.; Scott, R. L. Thermodynamic functions for nonelectrolyte solutions. *Ind. Eng. Chem.* **1963**, *55*, 43–46.